NOVEL STRATEGY FOR DRYING STUDIES – WHAT IF WE COULD SEE THE MOISTURE DISTRIBUTION INSIDE THE REFRACTORY CASTABLE?

M. H. Moreira[1]*, A. Tengattini[2], S. Dal Pont[3], V. C. Pandolfelli[1]

[1] Federal University of São Carlos, Graduate Program in Materials Science and Engineering, São Carlos, SP, Brazil

[2] Large Scale Structures, Institut Laue-Langevin, Grenoble, France

[3] 3SR, Universitè Grenoble Alpes, Grenoble, France

* murilo.moreira@estudante.ufscar.br

ABSTRACT

Refractory castables are a promising alternative to shaped products when considering its potential for reducing direct and indirect carbon dioxide emissions. However, their drying stage is usually an overconservative and long process that refrains the share of green potential of this class of refractories. To reduce the drying times, a throughout understanding of its fundamental mechanisms is required. Various studies have relied on indirect measurements of properties at laboratory conditions that are far from the industrial context. Others made use of sensors which present technical limitations and also affect the local readings. Thus, the current work depicts the use of neutron tomography as a valuable tool to study the drying of refractories, especially by using a ceramic casing which is proposed for providing unidirectional drying. Finally, this setup is also used to explore the effect of different heating rates on the drying of monolithics.

1 INTRODUCTION

Drying consists in the removal of water from a material via a gradient on the concentration, temperature or pressure distribution inside a porous medium[1]. Several mechanisms can act as a direct consequence of these inhomogeneities. The most notable example is the mass flux due to a pressure difference (i.e., following the Darcy law).

Even though several studies were carried out[1,2], the highly dynamic nature of the drying stage, as well as the large sizes and masses of refractory pieces applied in industrial processes,

still offer several challenges for the comprehension and, ultimately, the optimization of the drying performance of monolithics. Studies using thermogravimetric analysis provided important advances on the understanding of the dehydration reactions that take place during the initial heating of castables[1, 3, 4]. These tests, however, do not provide any information on the moisture distribution inside the material, or the pressure values which are developed in their pores. Additionally, several aspects need to be considered as well, such as the differences between the heating method used in the thermogravimetric analysis (TGA) furnaces and the ones for industrial process (i.e., heating from all sides or unidirectionally, using a gas burner or even microwaves), the size effects and the kinetics impact on the drying behavior.

Another approach is the use of sensors for the measurement of temperature and pressure evolution inside prismatic samples during unidirectional heating[5,6]. This method is often used to calibrate or even validate numerical models of Portland cement concrete under fire[2,5]. However, Dauti et al.[7] demonstrated, with the help of neutron tomography, that even very thin (0.25 mm in diameter) thermocouples can change the local microstructure of the sample. Consequently, a large variation of pressure values is usually obtained during the measurements carried out with pressure, temperature and mass (PTM) tests, as reported in the literature[7] which renders a no representative data of the materials' drying step.

Direct imaging techniques became recently very promising, both for studying refractory and Portland cement concrete[3]. The most common techniques are the X-ray and neutron tomography, ground penetrating radar (GPR), or nuclear magnetic resonance (NMR), each technique displaying a different set of advantages and drawbacks inherent from the very nature of these methods. In the case of neutron tomography, the results are based on the scattering of neutrons by the hydrogen atoms comprising the water molecules[8]. The X-ray beam, on the other hand, interacts with the electrons of the atoms and, consequently, its capacity to differentiate between regions rich or poor in water is less efficient than the neutron tomography technique[8] (see Figure 1 (d)). Meanwhile, the GPR approach relies on the fact that the electromagnetic waves propagating in a medium are reflected and scattered when a sudden change in electrical properties is found (which occurs when water is present). Nevertheless, this technique is more feasible even for bigger samples than the ones used in the tomography-based techniques but at a lower resolution and is not able to reconstruct the 3D representation of water distribution inside the sample.

On the other hand, NMR, which is based on the relaxation time of the nucleus of the hydrogen, can provide information on the configuration of the water molecules[9] (i.e., if they are located inside small or big pores). This comes at the expense of the capability of reconstructing the whole 3D domain. Also, although possible[10], simultaneous drying and NMR analysis is challenging and prone to inaccuracies, as the heating elements often have metallic parts which can interfere with the results and the relaxation time can be affected by the temperature[9]. A summary of the setup of these techniques used to study the drying is presented in Figure 1.

It is clear from (a) that the main difference between X-ray and neutron tomography is the beam source, which is more complex and more expensive for the latter as it relies on a nuclear reactor to provide the high intensity neutron beam. Also, based on the setup of the NMR (b) and GPR (c), it is possible to see that the resulting data is essentially 1D. Finally, from Figure 1 (d), it is evident that the higher scattering of neutrons by hydrogens results in a more pronounced contrast between the regions rich in water and dry areas, as seen from the radial slice.

Figure 1: Experimental layout of the imaging techniques, where (a) is the setup of the X-ray or neutron tomography, (b) represents the nuclear magnetic resonance tests and (c) describes the function of the ground penetrating radar. The comparison between neutron and X-ray can be seen in (d), where the difference of interaction of each element with the different sources is also presented. Adapted from Stelzner et al.[9], Felicetti et al.[7] and Dauti et al.[8].

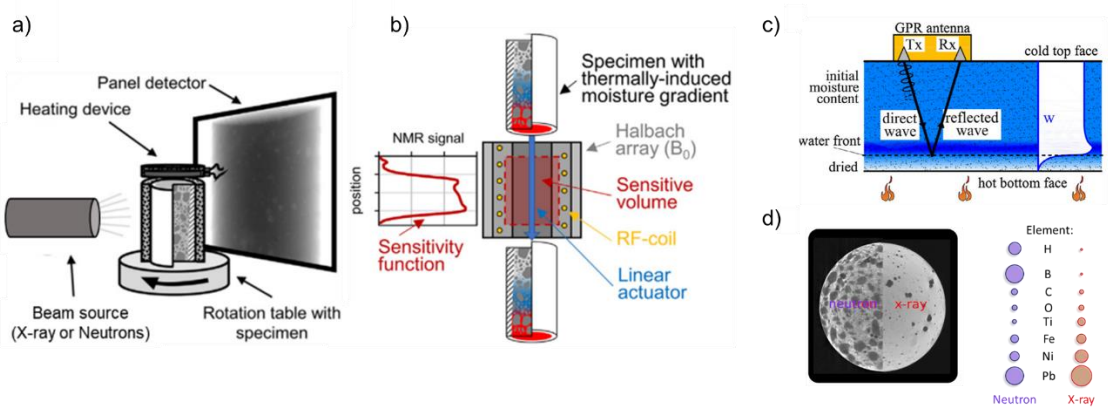

Thus, the neutron tomography analysis was chosen to be applied for studying refractories castables as a complement to the works carried out by Barakat et al.[9], which was based on using NMR. Consequently, the current study aims to present the very first (to the best of the authors' knowledge) direct observation of the drying in a refractory material using neutron tomography. This is an important advance as it can directly benefit the numerical models of refractory castable drying as well as provide insights for optimization of the industrial processes.

2 MATERIALS AND METHODS

2.1 Neutron Tomography Tests

The experiments presented in the current work were performed on the NeXT equipment at the Institut Laue Langevin (ILL) with a final spatial resolution of 160 μm and a time interval between tomographies of only 58.5 s. Figure 2 presents the layout of the experiment; further details can be found in Tengattini et al.[11] An infrared radiator heater (Elstein HTS - High Temperature Heater) was placed on the top surface of the sample and its heating followed two distinct protocols: (i) the “slow heating” where the sample was heated with a 10 °C/min rate until reaching 500 °C and (ii) a “fast heating” of 158 °C/min rate up to 500 °C (see Figure 8).

A dense CAC-bonded refractory castable was prepared (Table 1) as described by Luz et al.[12]. The samples were cast in cylindrical PVC molds or in a sintered alumina ceramic casing with an inner diameter of 33 mm and a height of 50 mm, depending on using or not of a casing during the neutron tomography test.

Table 1: 5CAC composition used for the neutron tomography tests based on the Andreasen’s particle packing model with q = 0.21.

Raw Materials		Composition (wt.%)
Tabular Alumina (D<6mm)	Almatis	74
Calcined and reactive alumina	CL370, Almatis	11
	CT3000SG, Almatis	10
Calcium Aluminate Cement	Secar 71, Imerys	5
Distilled Water		4.5
Dispersant	Castament FS60, Basf	0.2

Figure 2: (a) Layout of the neutron tomography test conducted in the NeXT equipment at Institut Laue Langevin (ILL) and (b) vertical slice of the reconstructed data.

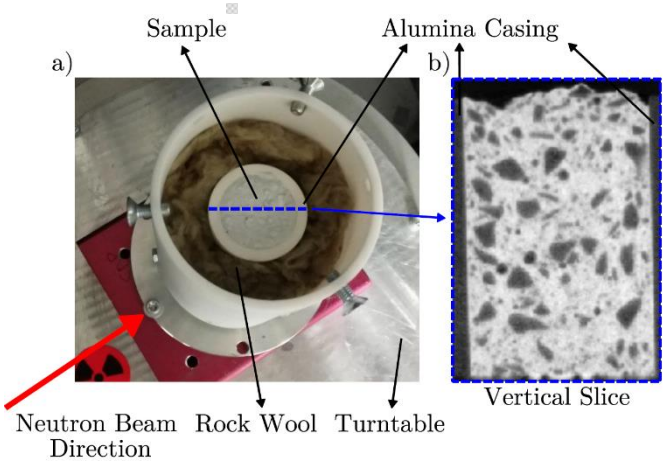

2.2 Post-processing of the Results

The 3D representation of the samples was obtained by using the Feldkamp filtered back projection and a commercial reconstruction software (X-act, by RX Solutions). The digital representation of the sample comprised a set of 300 slices in the cylinder's height. The basic quantity used for the analysis in the current work was the relative difference of voxel intensity, ψ(x,t), calculated by Equation 1.

$$\psi\ \mathbf{x},t\ = \frac{\left(I\ \mathbf{x},t\ - I\ \mathbf{x},t_0\ \right)}{I\ \mathbf{x},t_0} \times 100\% \qquad 1$$

where I(x,t) is the intensity of a voxel on position x (x=(x,y,z)) at time t, and I (x,t_0) is the voxel value at the reference state, which was defined to be the median of the first 10 tomographies, as described by Dauti et al.[8].

3 RESULTS AND DISCUSSION

3.1 Casing Effect Analysis

The first set of results describes the effect of a ceramic casing around the sample, which has several implications and can ultimately yield a truly unidirectional mass and heat transport inside the sample. Dauti et al.[8] reported that a noticeable increase in the water content was observed ahead of the drying front when evaluating Portland cement concrete samples with no impermeable ceramic casings. However, it was not identified whether such an increase was associated with real moisture accumulation or the "beam hardening" effect, which is the screening of more energetic neutrons by the hydrogen scattering at the water-rich positions, as it can mainly take place when lateral drying occurs.

Tengattini et al.[11], tried using quartz and titanium as the enclosing casing, which was not successful. This might be related to differences in the thermal expansion of the casing and the sample, resulting in some air gaps from where water could still escape (see Figure 5). Thus, the alumina ceramic casing used in the present work was specifically selected to match the characteristics of the 5CAC composition and result in a truly unidimensional drying.

Figure 3 describes the relative difference in the water distribution for samples with and without the ceramic casing. Three main conclusions can be readily drawn from these results: (i) the drying front is completely flat when the sample is cast inside the alumina casing; (ii) the water

accumulation is more evident in the sample inside the ceramic jacket and (iii) a secondary drying front is observed on the bottom of this sample.

Figure 3: Relative water content difference with respect to the initial state for samples with and without a ceramic casing for different time steps.

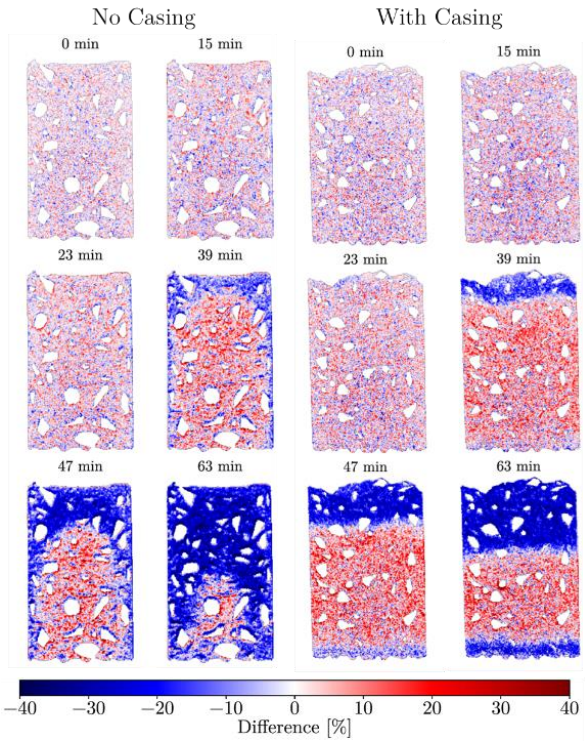

This set of results is important and confirms some observations as well as juxtaposes others. Firstly, the secondary drying is an important effect to be observed. Even in this case where the sample size was small, and numerical simulations indicated that the temperature gradient was around 17°C, this secondary drying is observed indicating that in real life applications, the care with weepholes and the properties at the cold surface of a given refractory lining can be an important way to guarantee a safe and efficient drying. As a matter of fact, in industrial equipment when the lining is being dried, an intense flow at the weepholes either as a liquid stream, or in some cases even as water jets, is observed.

The current findings are not in tune with the conclusions presented by Barakat et al.[10], as these authors only observed minor increases in the saturation content, and claimed that it could not be related to moisture clog, as the samples and the thermal gradients were too small.

As the NMR results can't be spatially visualized, one can only infer that the procedures taken by Barakat et al.[10] to enforce the unidimensional drying were not enough, due to the

different thermal expansion coefficient of the evaluated refractory castable and the PTFE beaker used as the casing for the NMR tests[10]. Figure 4 shows the linear expansion behavior of 5CAC castable and other materials that were used as casings during the drying measurements.

Figure 4: Linear thermal expansion of common material candidates for casings for non-intrusive methods. The results are normalized from 100°C. Adapted from [13, 14, 15].

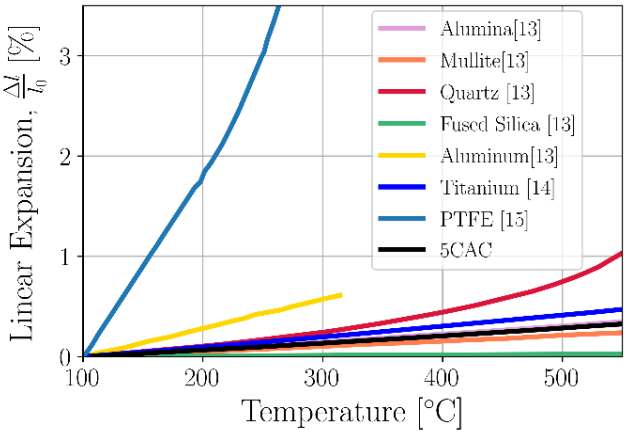

Moreover, the neutron tomography setup described herein can also be representative of a more realistic scenario due to the unidirectional nature of the mass and heat transport, as such conditions better represent the refractory lining of a furnace, for instance. This yields an important tool to not only explore alternatives to improve the efficiency of the drying of different compositions, but also to obtain a deeper understanding of the drying phenomenon itself.

3.1 Heating Rate Analysis

The second set of analysis was based on the comparison of the drying behavior of samples heated with different protocols. Two 5CAC samples were heated with a fast (158 °C/min) and slow (10 °C/min) rates until the heater temperature reached 500° C. The reason for these high heating rates was the limited time in the NeXT equipment. Further tests will consider heating rates closer to the ones found on the industrial application.

Figure 5 presents the heating curves scheduled for the infrared heater, as well as the results of the relative difference in the water content at different time steps. It is evident that the drying starts earlier for the sample heated with the 158 °C/min rate, where a noticeable drying front was detected with just 15 minutes of testing, when the heater temperature is already at 500 °C. On the other hand, the slow heated sample only shows a drying front at the 39-minute mark, when the temperature is still at 425 °C.

Figure 5: Relative water content difference with respect to the initial state for the samples heated using the fast and slow protocols. The dashed lines can be used to infer the temperature distribution on the sample by the infrared's temperature.

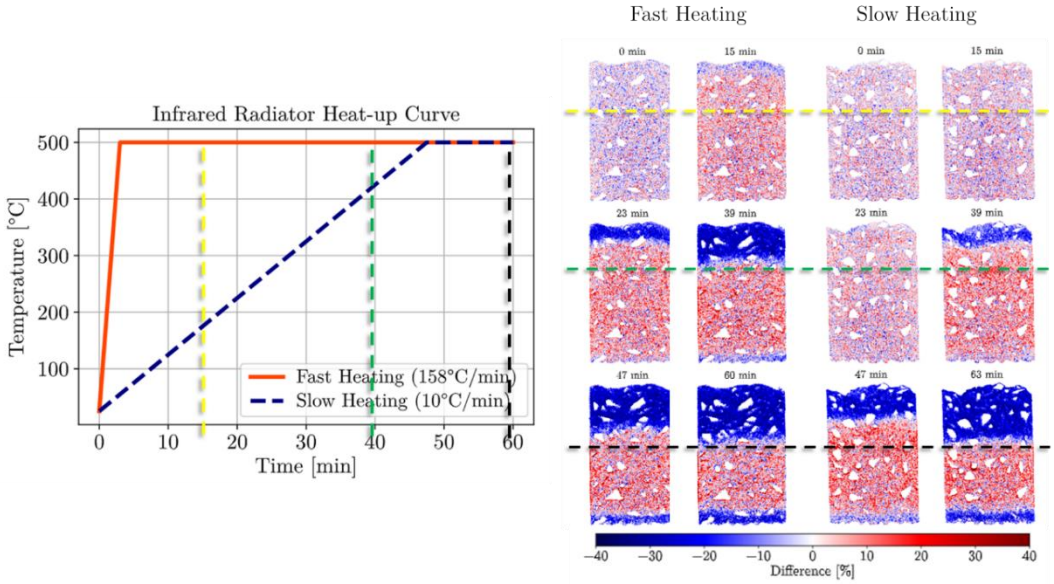

At the same time stage, the fast-heating procedure starts to show the development of a secondary drying front at the bottom of the sample. This is only clear for the slow heating sample at the 47-minute mark.

Most surprisingly is the fact that the final result at the end of the test is close for both heating conditions. This suggests that the temperature increase of the sample was very likely the limiting factor, especially when the heater reached the plateau stage and the sample's thermal conductivity became the regulating factor for the thermal energy transport.

Further studies with temperature measurements and with longer heating protocols are required to further understand this unexpected behavior. Nonetheless, these findings highlight the complexity of designing heating schedules and how the temperature plateaus need to be well understood and justified to result in safer drying process.

4 CONCLUSIONS

The drying of refractory castables is a complex subject which requires interdisciplinary efforts, ranging from numerical methods, experimental techniques and knowledge of the industrial perspective. Advanced non-intrusive techniques originally applied to Portland cement concrete can provide unprecedented findings. In the current work the use of neutron tomography yielded a novel method to study the castable drying.

The results pointed out that by using a ceramic casing completely altered the dynamics of water removal. The presence of a secondary drying front was also detected for the sample inside the casing, which displayed a pronounced moisture accumulation ahead of the drying front. When comparing two different drying rates, it was possible to see that using a temperature plateau at 500°C led to similar final water content.

The framework proposed herein can be further enhanced by using thermocouples to obtain the temperature profiles. Nevertheless, it should be reminded that this option will probably impact the local mass transport, but will only marginally affect the temperature distribution, yielding a scenario that represents the conditions faced by the neutron tomography tests. This would lead to reliable results which combined with those of neutron tomography would allow the moisture distribution to be correlated to the thermal state of the sample. Another alternative, would be to consider using longer heating protocols, that better represents the industrial scenario.

5 ACKNOWLEDGEMENTS AND FURTHER INFORMATION

This study was financed in part by the Coordenação de Aperfeiçoamento de Pessoal de Nível Superior - Brasil (CAPES) - Finance Code 001 and Fundação de Amparo à Pesquisa do Estado de São Paulo - FAPESP (grant number: 2021/00251-0 and 2019/07996-0). The authors are also greatly thankful for FIRE support in this work.

The results, discussions and most of the text of this article were based on the following publications: M.H. Moreira, S. Dal Pont, A. Tengattini, A.P. Luz, V.C. Pandolfelli, *Experimental proof of moisture clog through neutron tomography in a porous medium under truly one-directional drying*, J. Am. Ceram. Soc. vol. 105 (5) (2022) 3534–3543 (doi: 10.1111/jace.18297) and M.H. Moreira, S. Dal Pont, A. Tengattini, T. M. Cunha, R. F. Ausas, A.P. Luz, V.C. Pandolfelli, *Direct observation of drying by neutron and X-ray tomography analysis*. Proceedings of the UNITECR 2022. Therefore, for further details about its content, please consult the original papers.

6 REFERENCES

1. A.P. da Luz, M.A.L. Braulio, V.C. Pandolfelli, Refractory Castable Engineering, vol. 756, Goller Verlag GmbH, (2015)

2. Moreira, M. et al. Main trends on the simulation of the drying of refractory castables - Review. Ceramics International, Elsevier, vol. 47 [20] pp. 28086-28105 (2021)
3. A. P. da Luz et al., Drying behavior of dense refractory ceramic castables. Part 1– General aspects and experimental techniques used to assess water removal. Ceramics International, Elsevier, vol. 47 [16] pp. 22246-22268 (2021)
4. G. Palmer, et al. The accelerated drying of refractory concrete – Part 1: a review of current understanding, Refractories Worldforum 6 [2] pp 75–83 (2014)
5. K.G. Fey, et al., Experimental and numerical investigation of the first heat-up of refractory concrete, Int. J. Therm. Sci. [100] pp. 108-125, (2016)
6. P. Meunier, et. al, Methods to assess the drying ability of refractory castables, UNITECR 2013, pp.1–4 Kyoto, Japan. (2013)
7. Shen et al., On the moisture migration of concrete subject to high temperature with different heating rates, Cement and Concrete Research, [146], pp. 106492, (2021)
8. D. Dauti, A combined experimental and numerical approach to spalling of high performance concrete due to fire, Université Grenoble Alpes, (2018)
9. L. Stelzner et al., Thermally-induced moisture transport in high-performance concrete studied by X-ray-CT and 1HNMR, Construct. Build. Mater. pp. 600–609 (2019)
10. A.J. Barakat, et al., Direct observation of the moisture distribution in calcium aluminate cement and hydratable alumina-bonded castables during first-drying: an NMR study, J. Am. Ceram. Soc. pp. 2101–2113 (2020).
11. A. Tengattini, et al., Quantification of evolving moisture profiles in concrete samples subjected to temperature gradient by means of rapid neutron tomography: Influence of boundary conditions, hygro-thermal loading history and spalling mitigation additives, Strain [56] pp. 12371, (2020)
12. A.P. Luz, et al., Drying behavior optimization of dense refractory castables by adding a permeability enhancing active compound, Ceram. Int. pp. 9048–9060 (2019)
13. M. W. Barsoum, Fundamentals of ceramics, McGraw Hill, New York, (1997)
14. P. Hidnert, Thermal expansion of titanium, J. Res. Natl. Bur. Stand [30] pp. 101 (1943)
15. Characteristics of Fluororesins, Valqua LTDA, Available On-line on http://www.seal.valqua.co.jp/en/fp_property/fluoroplastics_characteristic/